



Effect of Column Diameter on the Performance of an Ion Exchange System in Reducing Water Hardness

Widya Yeni Rawati¹✉, Sunardi², Sri Widarti³, Sumarja⁴, Muhammad Nur Alim⁴

¹⁾ Jurusan Teknik Konversi Energi, Politeknik Negeri Bandung, West Java, Indonesia

²⁾ Jurusan Teknik Refrigerasi dan Tata Udara, Politeknik Negeri Bandung, West Java, Indonesia

³⁾ Jurusan Teknik Konversi Energi, Politeknik Negeri Bandung, West Java, Indonesia

⁴⁾ Jurusan Teknik Kimia, Politeknik Negeri Bandung, West Java, Indonesia

Abstract. Ion exchange is an effective method for removing hardness ions such as Ca^{2+} and Mg^{2+} from water, and its performance is strongly influenced by column design parameters. This study aims to evaluate the effect of column diameter on the efficiency of a sequentially operated cation–anion ion exchange system at a constant flow rate of 10 L/h. Six column diameters (20, 25, 30, 35, 40, and 50 mm) were tested using synthetic solutions. The results showed that the 30 mm column achieved the highest ion-exchange performance, with a removal efficiency of 92.47%. This column also produced the most well-defined breakthrough curve, yielding an exchange capacity of 8.76 mg/g, equivalent to 0.437 meq/g for Ca^{2+} and 0.720 meq/g for Mg^{2+} . These findings indicate that the 30 mm diameter provides an optimal balance between contact time and flow distribution, resulting in superior ion exchange efficiency.

Keywords: ion exchange, column diameter, column efficiency, Ca^{2+} , Mg^{2+}

Abstrak. Pertukaran ion merupakan metode yang efektif untuk menghilangkan ion penyebab kesadahan seperti Ca^{2+} dan Mg^{2+} dari air, dan kinerjanya sangat dipengaruhi oleh parameter desain kolom. Penelitian ini bertujuan untuk mengevaluasi pengaruh diameter kolom terhadap efisiensi sistem pertukaran ion kation–anion yang dioperasikan secara berurutan pada laju alir konstan sebesar 10 L/jam. Enam variasi diameter kolom (20, 25, 30, 35, 40, dan 50 mm) diuji menggunakan larutan sintetis. Hasil penelitian menunjukkan bahwa kolom berdiameter 30 mm memberikan kinerja pertukaran ion tertinggi dengan efisiensi penyisihan sebesar 92,47%. Kolom ini juga menghasilkan kurva *breakthrough* yang paling jelas, dengan kapasitas pertukaran sebesar 8,76 mg/g, yang setara dengan 0,437 meq/g untuk Ca^{2+} dan 0,720 meq/g untuk Mg^{2+} . Hasil ini menunjukkan bahwa diameter kolom 30 mm memberikan keseimbangan optimal antara waktu kontak dan distribusi aliran, sehingga menghasilkan efisiensi pertukaran ion yang lebih baik.

Kata kunci: pertukaran ion, diameter kolom, efisiensi kolom, Ca^{2+} , Mg^{2+}

Received: November 14, 2025, Accepted: January 5, 2026

Citation: Rawati, W.Y., Sunardi, S., Widarti, S., Sumarja., and Alim, M.N. (2025). Effect of Column Diameter on the Performance of an Ion Exchange System in Reducing Water Hardness. KOVALEN: Jurnal Riset Kimia, 11(2): 81-93.

INTRODUCTION

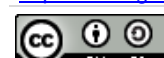
Water is an essential natural resource for both domestic and industrial activities (Achmad Fauzi et al., 2018). In industrial settings, it is commonly used for cleaning, heating, cooling,

and steam generation (Widarti, 2015). The quality of water used in these processes is highly important to ensure operational stability. One important indicator of water quality is its hardness level (Sahidin et al., 2024), which is mainly associated with the presence of calcium and magnesium ions. These ions occur

✉ Corresponding Author

E-mail: widya.yeni@polban.ac.id

<https://doi.org/10.22487/kovalen.2025.v11.i2.17907>



naturally in water bodies as a result of geological interactions with mineral-bearing rocks. Globally, hardness is a widespread issue, with more than 85% of freshwater sources classified as hard water (Yu et al., 2022). These ions tend to form insoluble deposits such as calcium carbonate and magnesium carbonate (Gao et al., 2023), which can accumulate in pipelines and equipment, causing scale formation (Maulizar et al., 2022). Such scaling reduces the effectiveness of industrial systems that rely on heat transfer. Over time, scale reduces heat transfer efficiency (Xing et al., 2020), leading to increased energy consumption and higher operational and maintenance costs. Therefore, managing water hardness is essential to maintain equipment performance and reduce operational losses.

Several treatment technologies have been developed to reduce water hardness, such as chemical precipitation, membrane filtration, and ion exchange (Xing et al., 2020). Among these methods, ion exchange is widely regarded as one of the most effective approaches for removing hardness ions. This process involves cross-linked, insoluble polymer resins that facilitate a stoichiometric exchange between ions in the solution and those attached to the resin matrix (Ahmer & Uddin, 2024). Because the resins can be regenerated and reused, ion exchange offers good efficiency and long-term economic benefits, making it suitable for continuous industrial applications.

The development of an ion exchange column system has been carried out by Kusumawati (Kusumawati et al., 2024), in which the ion exchange system was modified by adding an activated carbon column after the cation and anion resins. The results showed

that at an optimum flow rate of 0.6 GPM, a hardness reduction efficiency of up to 100% was achieved, with saturation times of 168 minutes for the cation resin and 46.4 minutes for the anion resin. This study emphasizes that operational parameters, particularly flow rate, play a crucial role in determining the ion exchange capacity of the resin and the overall performance of the system.

Another study conducted at flow rates ranging from 2.90–4.33 mL/s (10.44–15.59 L/h) and resin bed heights of 14 and 17 cm showed that the optimal condition was achieved at a flow rate of 4.33 mL/s with a column height of 14 cm, resulting in a hardness reduction efficiency of up to 93.56% (Nuryoto et al., 2024). Research on the effect of resin bed height has also been reported. Panjaitan (Panjaitan et al., 2023) demonstrated that using a resin bed height of 20 cm and an optimum flow rate of 50 mL/min in the treatment of chromium-containing wastewater resulted in a removal efficiency of 97.33%.

Although many studies have examined variations in flow rate and ion exchange column configurations, the influence of column dimensions—particularly column diameter—has received relatively little attention. Column diameter affects the linear flow velocity (Fekete et al., 2021), residence time (Syeda et al., 2025), and ion exchange efficiency (Rodrigues Reis & Hu, 2022). Differences in diameter also influence hydraulic head loss and fluid distribution within the resin bed (Quinn, 2014).

MATERIALS AND METHODS

Materials

The resins used consisted of the cation exchange resin Trilite KC-08 and the anion exchange resin Trilite MA-12. The synthetic

hard water sample was prepared using technical-grade CaCl_2 and MgCl_2 , while 0.01 N EDTA (Merck) was used as the titrant solution. For the regeneration process, 1 M NaOH and 1 M HCl (Merck) were employed.

Apparatus Design

The system consists of two resin columns arranged in series, namely a cation column followed by an anion column. Figure 1 presents a simple illustration of the ion exchange mechanism based on the experimental setup used in this study.

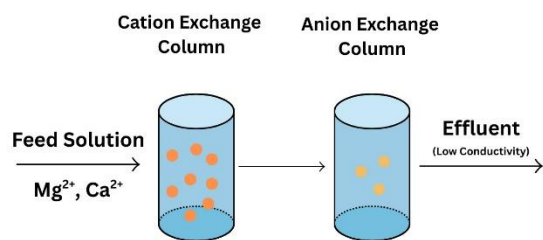


Figure 1. Simple illustration of the ion exchange mechanism

In the design of the ion exchange system, a dosing pump is used to maintain a stable flow rate (Marin et al., 2024), which is monitored using a flowmeter. Each column is constructed from acrylic tubing due to its high transparency, lightweight properties, and ease of modification for various fittings and connections (Zaokari et al., 2020).

The column diameter variations used were 20 mm, 25 mm, 30 mm, 35 mm, 40 mm, and 45 mm, with a total column length of 30 cm and a fixed resin bed height of 15 cm. The bottom section of each column was equipped with a mesh layer to prevent resin leakage. The piping system was fitted with control valves to regulate flow rate and direction, and flexible tubing was used as connectors between components. The entire unit was mounted on a PVC base supported by a hollow steel frame to ensure stability, ergonomic operation, and ease of relocation during laboratory use (Figures 2 and 3).

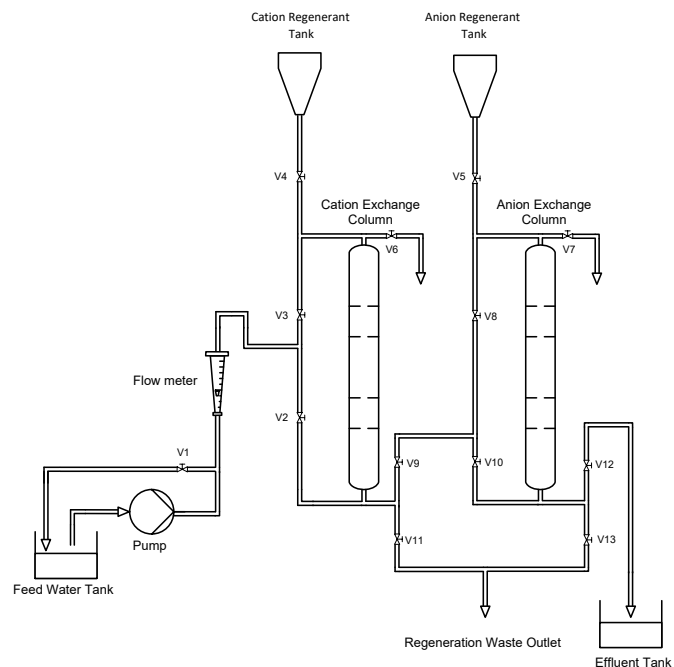


Figure 2. Ion exchange column system design



Figure 3. Ion exchange apparatus

Instrumentation

The supporting equipment used included a digital conductivity meter (Hanna HI9813-6), an analytical balance (Kern ABS 220-4), and standard glassware for sample collection and hardness titration.

Procedure

Sample preparation

The artificial water sample was prepared by dissolving $MgCl_2$ and $CaCl_2$ in 40 liters of tap water.

Ion exchange apparatus preparation

The resins were prepared by weighing the cation and anion exchange resins, which were

then soaked in 1 N HCl or 1 N NaOH solution, respectively, for 1 hour for activation (Brožová et al., 2015). The resins were subsequently rinsed with distilled water until a neutral pH was achieved. Afterward, the resins were packed into their respective columns, followed by a backwashing step (Shahab & Setiorini, 2023), in which water flows from the bottom to the top (Figure 4) to ensure complete resin wetting and to prevent channeling. Channeling is a phenomenon where the feed solution forms preferential flow paths, thereby reducing contact between the feed and the entire resin bed (Koch et al., 2023).

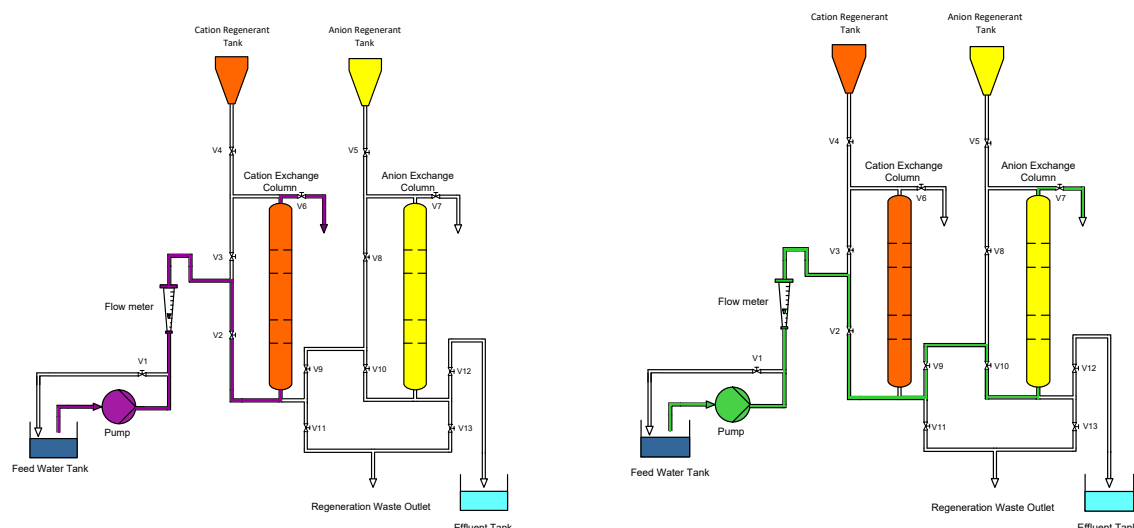


Figure 4. Schematic of cation backwash (left) and anion backwash (right)

Water treatment process

The water treatment sequence, or service flow, as shown in Figure 5, begins with the feed tank, from which water is pumped toward the flowmeter. The water then enters the cation column, flowing from top to bottom. In this column, Ca^{2+} and Mg^{2+} ions are exchanged with H^+ ions released by the cation resin. The water subsequently flows into the anion column,

moving from bottom to top, where anions such as Cl^- and SO_4^{2-} are exchanged with OH^- ions provided by the anion resin. The treated water then exits through the outlet into the effluent tank. Through this ion exchange mechanism, the concentrations of both cations and anions in the water are significantly reduced, resulting in improved water quality compared to the original feed water.

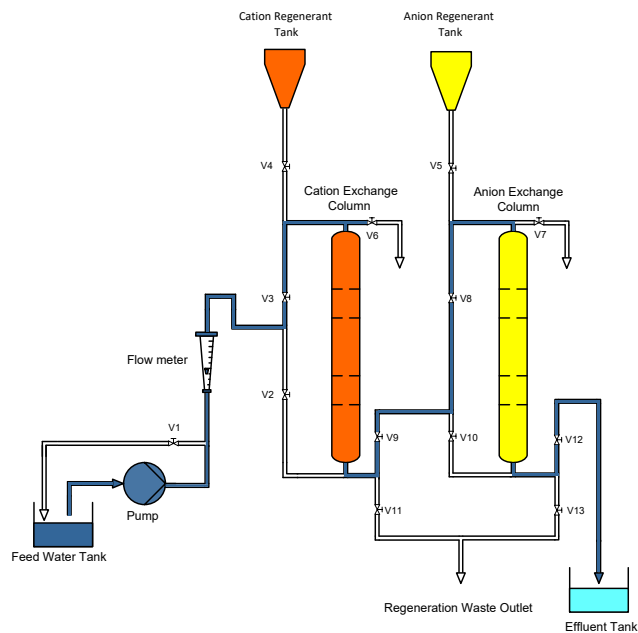


Figure 5. Schematic of the water treatment flow

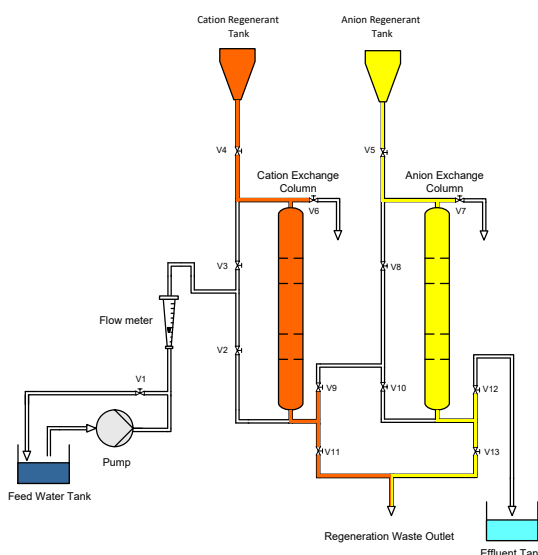


Figure 6. Schematic of the cation regeneration flow (orange) and anion regeneration flow (yellow)

After the water treatment process, the resin becomes saturated and loses its optimal ion exchange capacity. To restore the resin capacity, a regeneration step is carried out (Chandrasekara & Pashley, 2015), in which the resin is washed with a regenerant solution so that it returns to its active form and can be reused. The regeneration scheme is shown in Figure 6.

RESULT AND DISCUSSION

Resin Efficiency and Conductivity Measurement

To examine the effect of column diameter, the resin bed height was kept constant. This arrangement was intended to maintain a consistent mass transfer zone and contact time, ensuring that any observed differences were solely due to variations in column diameter (Gebauer et al., 2003). By maintaining the same resin bed height, the influence of other factors such as adsorption capacity and breakthrough time could be minimized. Consequently, the comparison becomes more

valid and accurately reflects the effect of column diameter (Chromatographyonline, n.d.).

The amount of cation and anion resin in each column was determined based on the effective column volume, calculated using the cylindrical volume equation. The mass of the resin was obtained by multiplying the resin volume by its density, with the cation resin density being 1.29 g/mL (Trilite KC-08, 2025) and the anion resin density being 1.09 g/mL (Trilite MA-12, n.d.). Effluent samples were collected every 200 mL up to a total volume of 4 L to measure conductivity and hardness concentration using the complexometric titration method (Kusumawati et al., 2024). The experimental data obtained are presented in Table 1.

Table 1 shows the changes in hardness and conductivity after the ion exchange process at various column diameters. In general, increasing the column diameter results in greater reductions in both hardness and conductivity, with the highest efficiency achieved at a diameter of 30 mm.

Table 1. Effect of column diameter on hardness removal and conductivity

Column Diameter (mm)	Initial Hardness (mg/L as CaCO ₃)	Average Hardness (mg/L as CaCO ₃)	Efficiency (%)	Initial Conductivity (mS/cm)	Final Conductivity (mS/cm)
20	324	28.8	91.11	0.87	0.71
25	324	25.4	92.16	0.87	0.31
30	324	24.6	92.47	0.87	0.10
35	324	27.0	91.67	0.87	0.43
40	324	26.8	91.73	0.87	0.38
50	324	27.2	91.60	0.87	0.71

Figure 7 presents the hardness reduction efficiency curves for the different column diameters. It can be observed that all column diameter variations show a sharp decrease in

hardness at low effluent volumes (<0.5 L), followed by stabilization in the range of 10–30 mg/L up to 4 L of effluent. This indicates that the resin had not yet reached its saturation point

(breakthrough point). The column with a diameter of 30 mm exhibited the best performance, characterized by the fastest decrease in hardness and the lowest stable

hardness value. In contrast, smaller diameters, such as 20 mm, showed poorer stability, suggesting non-uniform flow distribution.

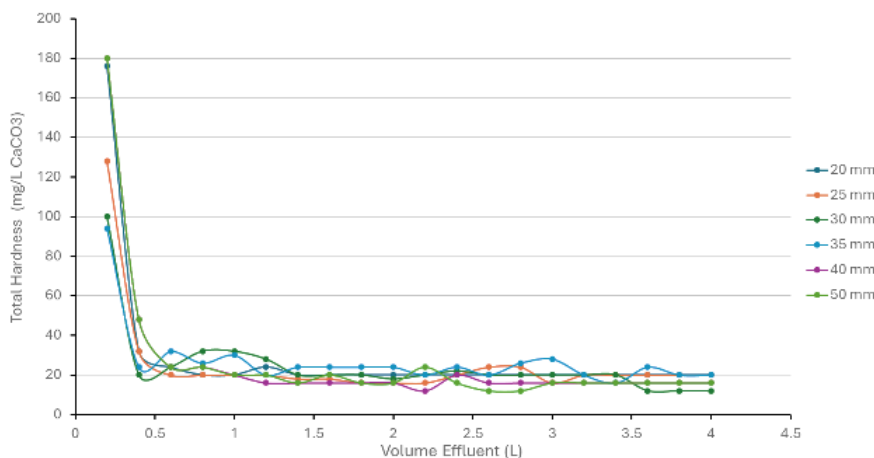


Figure 7. Curve of hardness as a function of effluent volume

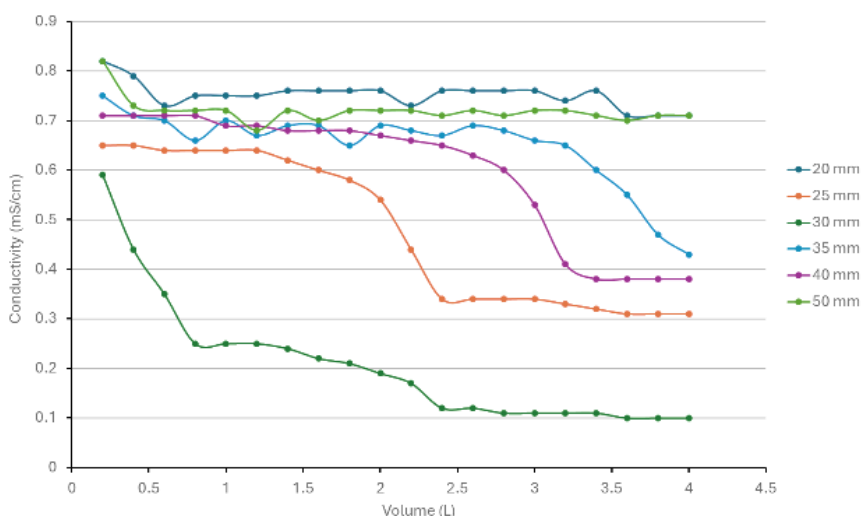


Figure 8. Relationship between effluent conductivity and effluent volume

The reduction in hardness in the effluent is attributed to the ion exchange process between the Ca^{2+} and Mg^{2+} ions responsible for hardness and the H^+ or Na^+ ions on the ion exchange resin. A similar phenomenon was reported by Li et al. (2016), who demonstrated that the ion exchange process effectively reduces water hardness by removing calcium and magnesium ions. A more recent study by Gholami et al. (Nasrollahi et al., 2025) also

emphasized that hardness removal efficiency is strongly influenced by column characteristics, including diameter and resin volume.

To observe changes in water quality based on another parameter, the conductivity versus effluent volume curve is shown in Figure 8. The decrease in effluent conductivity indicates a reduction in the total dissolved ions due to the ion exchange process occurring in the resin. This phenomenon is consistent with the

findings of Petrov et al. (2022), who explained that solution conductivity decreases as charged ions are removed through ion exchange in cation and anion resins.

The 30 mm diameter column exhibited the most significant decrease in conductivity, from approximately 0.6 mS/cm to below 0.1 mS/cm at a volume of 4 L, because its diameter creates optimal hydraulic conditions for ion exchange. At this diameter, the linear flow rate is sufficiently low to allow adequate contact time between the solution and the resin, while the flow pattern remains uniform across the bed. This combination minimizes mass-transfer limitations and ensures effective resin utilization. The 25 mm diameter column also showed a considerable reduction in conductivity, although not as substantial as that of the 30 mm column. Meanwhile, the 35 mm and 40 mm diameter columns experienced only moderate reductions.

The similarity in conductivity values observed in the 20 mm and 50 mm column diameters can be attributed to two key phenomena: rapid flow rate and channeling. In the 20 mm column, the small cross-sectional area results in a higher linear velocity at the same volumetric flow rate. This rapid flow reduces the contact time between the solution and the resin, causing insufficient ion exchange and leading to higher effluent conductivity. Conversely, in the 50 mm column, the larger diameter promotes non-uniform flow distribution. This condition often leads to channeling, where the solution preferentially flows through certain paths with lower resistance instead of being evenly dispersed across the resin bed. Channeling reduces effective resin utilization because a portion of the resin does not actively participate in the

exchange process. As a result, the overall ion removal efficiency decreases, producing conductivity values similar to those in the 20 mm column.

As previously discussed, the hardness removal values for the different column diameters showed only minor variations, indicating that all columns were generally capable of reducing Ca^{2+} and Mg^{2+} concentrations to a similar extent. In contrast, the conductivity values demonstrated clearer differences, which more accurately reflect the ion exchange performance under each hydraulic condition. Conductivity is more sensitive to residual ions in the effluent, including ions that are not classified as hardness but still contribute to the total ionic strength. Therefore, focusing on conductivity allows a better assessment of how column diameter influences mass transfer, contact time, and flow uniformity. Columns with suboptimal diameters either experience reduced contact time due to high linear velocities or exhibit channeling, both of which result in higher conductivity despite similar hardness values. This explains why conductivity serves as a more reliable performance indicator than hardness alone in this system.

Based on the hardness removal results discussed earlier, treatment efficiency was calculated to quantitatively evaluate the performance of each column diameter. To determine the extent of the column's effectiveness in reducing ion concentrations, treatment efficiency was calculated based on ion concentrations before and after the ion exchange process. The efficiency data in Table 1 were calculated using Equation (1) (Nuryoto et al., 2024).

$$\text{Efficiency (\%)} = \frac{C_0 - C_e}{C_0} \times 100$$

The efficiency values for each column diameter variation are shown in Figure 9.

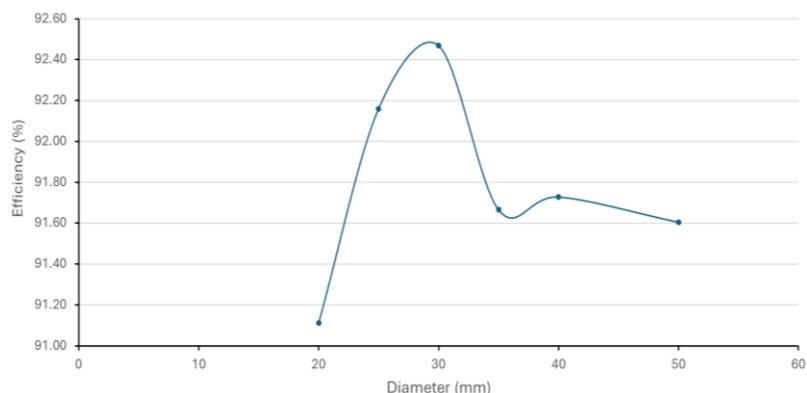


Figure 9. Hardness removal efficiency as a function of column diameter

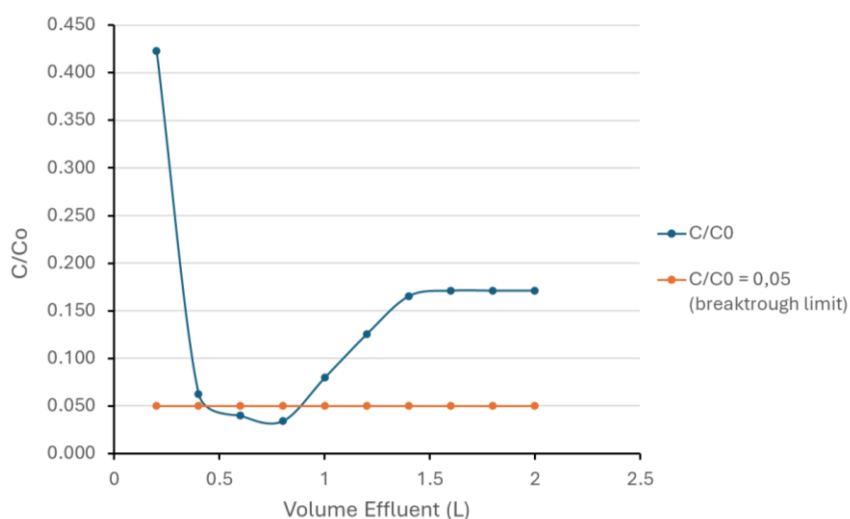


Figure 10. Breakthrough curve at 30 mm diameter

Breakthrough Curve and Resin Capacity

Since the effluent volume in this experiment was limited to only 4 L, the resin saturation phenomenon (breakthrough) could not be clearly observed. To obtain a more comprehensive breakthrough profile, a follow-up experiment was performed using the 30 mm diameter column with a more concentrated sample solution, namely 700 mg/L.

The curve in Figure 10 shows that the C/C_0 ratio gradually increases with increasing effluent volume, and the breakthrough point is

determined at $C/C_0 = 0.05$, in accordance with common criteria in ion exchange studies (Lima et al., 2024). Theoretically, a breakthrough curve exhibits a sigmoidal (S-shaped) form that indicates three main zones: the unsaturated zone, the mass transfer zone, and the saturated zone (Dima et al., 2024). However, in this experiment, the resulting curve does not fully form an ideal S-shape. This condition is likely caused by flow non-uniformity during the initial operation of the column, and the system not yet reached complete saturation.

Table 2. Ion exchange capacity of the resin in the 30 mm diameter column

Volume (L)	C (mg/L)	C ₀ (mg/L)	(C ₀ -C) x ΔV	Q mg/g	Q Ca ²⁺ (meq/g)	Q Mg ²⁺ (meq/g)
0.2	296	700	80.8	0.59	0.029	0.049
0.4	44	700	131.2	1.55	0.077	0.128
0.6	28	700	134.4	2.53	0.126	0.208
0.8	24	700	135.2	3.52	0.176	0.290
1.0	56	700	128.8	4.46	0.223	0.367
1.2	88	700	122.4	5.36	0.267	0.441
1.4	116	700	116.8	6.21	0.310	0.551
1.6	120	700	116	7.06	0.352	0.581
1.8	120	700	116	7.91	0.395	0.651
2.0	120	700	116	8.76	0.437	0.720

The ion exchange capacity (Q) of the resin in the 30 mm diameter column is calculated using Equation (2) (He et al., 2020):

$$Q = \frac{\sum(C_0 - C) \times \Delta V}{m}$$

where C₀ and C are the initial concentration and the effluent concentration (mg/L), respectively, V is the effluent volume (L), and m is the mass of the resin (136.71 g). The value of Q represents the amount of ions exchanged per unit mass of resin. Based on Table 2, the ion exchange capacity of the resin increases with increasing effluent volume, approaching the saturation point at around 2 L. The total resin capacity obtained is 8.76 mg/g, which is equivalent to 0.437 meq/g for Ca²⁺ ions and 0.720 meq/g for Mg²⁺ ions. According to the technical data sheet from Samyang Corporation, the cation resin Trilite KC-08 has a total capacity of 1.9–2.1 meq/mL, while the anion resin Trilite MA-12 has a total capacity of 1.3–1.4 meq/mL.

The capacity values obtained in this study (0.437–0.720 meq/g) indicate that the utilization of active sites in the resin has only reached approximately 9–15% of the total capacity. This

condition suggests that the ion exchange process occurred mainly within a limited portion of the mass transfer zone, meaning not all layers of the resin participated optimally. It can also be influenced by the initial ionic form of the resin (Na⁺ or H⁺) and the regeneration conditions, which significantly affect the resin's ability to exchange Ca²⁺ and Mg²⁺ ions. Flow distribution in the column, variations in column diameter, bed porosity, and flow rate can cause uneven flow (channeling), which shortens the contact time between ions and the active sites of the resin. Competition between Ca²⁺ and Mg²⁺ ions in the solution also plays a role, as both ions compete for the same sites on the resin surface.

This is consistent with the findings of Mountadar (Mountadar et al., 2018), who reported that the Duolite C206A resin has a maximum exchange capacity of approximately 20–30 mg/g for Ca²⁺ and Mg²⁺; however, the actual capacity in a dynamic column system is much lower due to limitations in diffusion and flow distribution.

Overall, the results of this study indicate that the cation–anion ion exchange column

system performs reasonably well, but there remains potential for further optimization of operational conditions, such as flow rate, regenerant concentration, or column length, in order to achieve closer to maximum performance of the resin media.

CONCLUSION

This study demonstrates that variations in column diameter have a significant effect on the efficiency of the ion exchange process in the ion exchange system. Among the five variations tested, the column with a diameter of 30 mm exhibited the most optimal performance, achieving an efficiency of 92.47%. In this column, a clear breakthrough curve was observed, with an ion exchange capacity of 8.76 mg/g, which is equivalent to 0.437 meq/g for Ca^{2+} ions and 0.720 meq/g for Mg^{2+} ions.

ACKNOWLEDGMENT

The authors gratefully acknowledge the support of Sistem Informasi Manajemen Penelitian dan Pengabdian Pada Masyarakat (SIPPM) POLBAN and the contributions of fellow researchers during the data collection and analysis stages of this study.

REFERENCES

Achmad Fauzi, L., Yutrisya, A., Rachmatiyah, N., Sapanli, K., Ekonomi Sumberdaya dan Lingkungan, D., Ekonomi dan Manajemen, F., & Pertanian Bogor, I. (2018). *Prosiding Seminar Nasional Hari Air Dunia*.

Ahmer, M. F., & Uddin, M. K. (2024). Structure properties and industrial applications of anion exchange resins for the removal of electroactive nitrate ions from contaminated water. *RSC Advances*, 14(45), 33629–33648. <https://doi.org/10.1039/D4RA03871A>

Brožová, L., Křivčík, J., Neděla, D., Kysela, V., & Žitka, J. (2015). The influence of activation of heterogeneous ion-exchange membranes on their electrochemical properties. *Desalination and Water Treatment*, 56(12), 3228–3232. <https://doi.org/10.1080/19443994.2014.980975>

Chandrasekara, N. P. G. N., & Pashley, R. M. (2015). Study of a new process for the efficient regeneration of ion exchange resins. *Desalination*, 357, 131–139. <https://doi.org/10.1016/J.DESAL.2014.11.024>

Chromatographyonline. (n.d.). Retrieved October 23, 2025, from https://www.chromatographyonline.com/view/effects-column-inner-diameter-and-packed-bed-heterogeneities-chromatographic-performance?utm_source=chatgpt.com

Dima, J. B., Ferrari, M. A., & Zaritzky, N. (2024). Mathematical modeling of breakthrough curves in dynamic column adsorption: analytical solutions and validation. *Journal of Engineering Mathematics*, 147(1). <https://doi.org/10.1007/S10665-024-10375-X>

Gao, M., Yang, Z., Liang, W., Ao, T., & Chen, W. (2023). Recent advanced freestanding pseudocapacitive electrodes for efficient capacitive deionization. *Separation and Purification Technology*, 324, 124577. <https://doi.org/10.1016/J.SEPPUR.2023.124577>

Gebauer, K. H., Luo, X. L., Barton, N. G., & Stokes, A. N. (2003). Efficiency of preparative and process column distribution systems. *Journal of Chromatography A*, 1006(1–2), 45–60. [https://doi.org/10.1016/S0021-9673\(03\)00177-8](https://doi.org/10.1016/S0021-9673(03)00177-8)

He, H., Huang, Y., Yan, M., Xie, Y., & Li, Y. (2020). Synergistic effect of electrostatic adsorption and ion exchange for efficient removal of nitrate. *Colloids and Surfaces A: Physicochemical and Engineering Aspects*, 584, 123973. <https://doi.org/10.1016/J.COLSURFA.2019.123973>

Koch, J., Scheps, D., Gunne, M., Boscheinen, O., & Frech, C. (2023). Mechanistic

modeling of cation exchange chromatography scale-up considering packing inhomogeneities. *Journal of Separation Science*, 46(9), 2300031. <https://doi.org/10.1002/JSSC.202300031>;PAGE:STRING:ARTICLE/CHAPTER

Kusumawati, E., Jayanti, R. D., Putri, L. H., Annisa, N., & Paramitha, T. (2024). Evaluasi dan Modifikasi Alat Penukar Ion dengan Penambahan Kolom Adsorpsi Karbon Aktif untuk Menurunkan Kesadahan: KOVALEN: *Jurnal Riset Kimia*, 10(1), 1–10. <https://doi.org/10.22487/kovalen.2024.v10.i1.16556>

Li, J., Koner, S., German, M., & Sengupta, A. K. (2016). Aluminum-Cycle Ion Exchange Process for Hardness Removal: A New Approach for Sustainable Softening. *Environmental Science & Technology*, 50(21), 11943–11950. <https://doi.org/10.1021/ACS.EST.6B03021>

Marin, N. M., Nita Lazar, M., Popa, M., Galaon, T., & Pascu, L. F. (2024). Current Trends in Development and Use of Polymeric Ion-Exchange Resins in Wastewater Treatment. *Materials 2024, Vol. 17, Page 5994*, 17(23), 5994. <https://doi.org/10.3390/MA17235994>

Maulizar, A., Masykur, M., & Supardi, J. (2022). Analisis pH, TDS, Total Hardness, Alkalinity, Dan Silica Pada Boiler Feet Water di PT. SOCFINDO Perkebunan Kelapa Sawit di Seunagan. *Jurnal Mekanova: Mekanikal, Inovasi Dan Teknologi*, 8(1), 129. <https://doi.org/10.35308/JMKN.V8I1.5630>

Mountadar, S., Hayani, A., Rich, A., Siniti, M., & Tahiri, S. (2018). Equilibrium, kinetic, and thermodynamic studies of the Ca²⁺ and Mg²⁺ ions removal from water by Duolite C206A. *Solvent Extraction and Ion Exchange*, 36(3), 315–329. <https://doi.org/10.1080/07366299.2018.1478369>

Nasrollahi, Y., Khoshravesh, M., & Aghajani Mazandarani, G. (2025). New improvement ion exchange treatment method for drinking water in Juybar City, Iran. *Applied Water Science*, 15(7), 1–15. <https://doi.org/10.1007/S13201-025-02551-W/FIGURES/7>

Nuryoto, N., Hartono, R., & Rahmayetty, R. (2024). Pengolahan Air Menggunakan Proses Demineralisasi dengan Memanfaatkan Resin Penukar Ion: Studi Pengaruh Laju Alir dan Tinggi Resin. *Jurnal Ilmu Lingkungan*, 22(2), 393–400. <https://doi.org/10.14710/JIL.22.2.393-400>

Panjaitan, L., Putri, M. S., & Pujiastuti, C. (2023). Pengaruh Laju Alir Terhadap Penurunan Kadar Logam Berat Cr pada Limbah Industri Batik dengan Metode Ion Exchange Menggunakan Resin Amberlite IR 120Na. *Enviroous*, 4(1), 1–4. <https://doi.org/10.33005/ENVIROUS.V4I1.149>

Petrov, O., Iwaszcuk, N., Bejanidze, I., Kharebava, T., Pohrebennik, V., Didmanidze, N., & Nakashidze, N. (2022). Study of the Electrical Conductivity of Ion-Exchange Resins and Membranes in Equilibrium Solutions of Inorganic Electrolytes. *Membranes*, 12(2), 243. <https://doi.org/10.3390/MEMBRANES12020243>

Quinn, H. M. (2014). A Reconciliation of Packed Column Permeability Data: Deconvoluting the Ergun Papers. *Journal of Materials*, 2014(1), 548482. <https://doi.org/10.1155/2014/548482>

Rodrigues Reis, C. E., & Hu, B. (2022). Volumetric Scale-Up of a Packed-Bed Ion-Exchange System to Extract Phytate from Thin Stillage. *Membranes*, 12(2), 230. <https://doi.org/10.3390/MEMBRANES12020230/S1>

Sahidin, S., Aba, L. A., Eso, R., Okto, A., Okto, A., Alfirman, A., & La Ode Andimbara. (2024). Analysis of Lime Content (CaCO₃) in Clean Water Sources in Tampo Village, Napabalano District, Muna Regency. *Jurnal Rekayasa Geofisika Indonesia*, 6(01), 51–61. <https://doi.org/10.56099/jrgi.v6i01.69>

Shahab, A., & Setiorini, I. A. (2023). Efektifitas Volume Resin Ion Exchanger Terhadap Kapasitas Pertukaran Ion dan Waktu Jenuh Pada Unit Demin Plant di PT PLN (PERSERO) UPDK Keramasan. *Journal of Innovation Research and Knowledge*, 2(9), 3791–3802. <https://doi.org/10.53625/JIRK.V2I9.5407>

Syeda, H. I., Muthukumaran, S., & Baskaran, K. (2025). Dynamic adsorption of heavy metals on functionalized and regeneratable biopolymeric aerogels: Fixed-bed column reactor modelling and dual functionality elution technique. *Separation and Purification Technology*, 363, 131861. <https://doi.org/10.1016/J.SEPPUR.2025.131861>

Trilite KC-08. (2025). <https://eclim.vn/uploads/images/Specifications/TRILITE-KC-08.pdf>

Trilite MA-12. (n.d.). Retrieved October 29, 2025, from www.lennotech.comFax.

Widarti, S. (2015). The Influence of Feed Flow Rate Toward Capacity of Commercial Cation Exchanger Resin and Adsorption Of Metal Ion With Different Valence. *SIGMA-Mu*, 7(1), 1-6. <https://doi.org/10.35313/sigmamu.v7i1.833>

Wu, N., & Bradley, A. C. (2012). Effect of column dimension on observed column efficiency in very high pressure liquid chromatography. *Journal of Chromatography A*, 1261, 113–120. <https://doi.org/10.1016/J.CHROMA.2012.05.054>

Xing, W., Liang, J., Tang, W., He, D., Yan, M., Wang, X., Luo, Y., Tang, N., & Huang, M. (2020). Versatile applications of capacitive deionization (CDI)-based technologies. *Desalination*, 482, 114390. <https://doi.org/10.1016/J.DESAL.2020.114390>

Yu, F., Yang, Z., Cheng, Y., Xing, S., Wang, Y., & Ma, J. (2022). A comprehensive review on flow-electrode capacitive deionization: Design, active material and environmental application. *Separation and Purification Technology*, 281, 119870. <https://doi.org/10.1016/J.SEPPUR.2021.119870>

Zaokari, Y., Persaud, A., & Ibrahim, A. (2020). Biomaterials for Adhesion in Orthopedic Applications: A Review. *Engineered Regeneration*, 1, 51–63. <https://doi.org/10.1016/j.engreg.2020.07.002>